UPPSALA
UNIVERSITET

UPTEC X 16 027
Examensarbete 30 hp
September 2016

Site-specific labelling of anti-HER2 ADAPT proteins for molecular imaging applications

Jessica Lövgren

UPPSALA UNIVERSITET

Degree Project in Molecular Biotechnology

Masters Programme in Molecular Biotechnology Engineering,
Uppsala University School of Engineering

UPTEC X 16 027	**Date of issue 2016-09**

Author

Jessica Lövgren

Title (English)

Site-specific labelling of anti-HER2 ADAPT proteins for molecular imaging applications

Abstract

Cancer is one of the leading causes of death worldwide. It is of great importance to use reliable diagnostic methods before determining treatment methods. Molecular imaging is a non-invasive approach of visualising tumours *in vivo*. This method requires imaging agents that are detectable and binds specifically to the tumour. The aim of this degree project was to produce and characterise a protein-based imaging agent, called ADAPT, that has been engineered to bind the breast cancer associated receptor HER2. This protein has previously been labelled with radionuclides in the N-terminal and tested *in vivo* with promising results. However, due to the fact that the position of the radiolabel can affect the biodistribution of the imaging agent, a comparison to C-terminal radiolabelled variants is of high interest. Radiolabelling can be performed by first attaching a chelator to the protein and later bind the radionuclide through the chelator. The chelator used in this project binds to a thiol group and therefore a unique cysteine was added to the C-termini. The N-termini were altered to both generate variants with and without purification tag. Proteins with altered N-termini and C-termini were produced and later characterised by circular dichroism and surface plasmon resonance. None of the non-tagged variants could be produced to a sufficient amount and was discarded for further studies. However, all variants with a purification tag could be produced and the shortest variant was chosen to be tested *in vivo*.

Keywords

cancer diagnostics, molecular imaging, ADAPT, HER2

Supervisors

Sophia Hober
KTH

Scientific reviewer

Fredrik Frejd
Uppsala University

Project name	Sponsors Vetenskapsrådet, Cancerfonden
Language **English**	Security
ISSN 1401-2138	Classification
Supplementary bibliographical information	Pages **29**

Biology Education Centre Biomedical Center Husargatan 3, Uppsala
Box 592, S-751 24 Uppsala Tel +46 (0)18 4710000 Fax +46 (0)18 471 4687

Site-specific labelling of anti-HER2 ADAPT proteins for molecular imaging applications

Jessica Lövgren

Populärvetenskaplig sammanfattning

Cancer är en sjukdom som påverkar människor världen över. Det är en av de största dödsorsakerna hos människor och antalet årliga fall förväntas att öka. Ökningen beror dels på att världens befolkning ökar och åldras, men också att människor i utvecklingsländer övergår till livsstilar som ger ökad cancerrisk.

Korrekt diagnostik är viktigt för att kunna ge patienter rätt behandling. Ett sätt att diagnostisera cancer är att använda molekylär bildtagning, där tumörer visualiseras genom att detektera en bildtagningsmolekyl som binder till en markör på cancercellen. ADAPTs är en grupp av små proteinmolekyler som har designats för att kunna binda olika markörer med hög affinitet. *In vivo*-studier har utförts där ADAPT har använts som bildtagningsmolekyl, vilket har visat lovande resultat. Det finns dock ett intresse av att undersöka om dessa bildtagningsmolekyler kan förbättras ytterligare för att minimera upptag i friska organ och på så vis öka tumör-till-organ koncentrationsförhållanden av radioaktiviteten. I tidigare studier har proteinerna blivit inmärkta med radionuklider i N-terminalen. Då positionen av radioinmärkningen kan påverka biodistributionen behövs en jämförelse mot varianter med radioinmärkt C-terminal.

Syftet med det här examensarbetet var att producera och karakterisera ADAPT-varianter för inmärkning med radionuklider i C-terminalen. Karakteriseringen inkluderade analys av stabilitet, sekundärstruktur och bindningskapacitet till markören HER2, en receptor som har ökat uttryck hos vissa cancertumörer. Målet med de producerade ADAPT-varianterna är att analysera dem *in vivo* för jämförelse mot tidigare testade varianter. Jämförelsen syftar till att undersöka om biodistributionen kan förbättras genom att flytta radioinmärkningen.

Examensarbete 30 hp

Civilingenjörsprogrammet i molekylär bioteknik

Uppsala universitet, september 2016

CONTENTS

LIST OF ABBREVIATIONS AND ACRONYMS 7
1 INTRODUCTION 9
1.1 Background 9
1.1.1 Albumin binding domain and ADAPT 9
1.1.2 Human epidermal growth factor receptor 2 and ADAPT6 10
1.1.3 Molecular imaging 10
1.2 Aims and objectives 11
2 MATERIAL AND METHODS 12
2.1 Protein production 12
2.1.1 Cloning 12
2.1.2 Protein production 12
2.1.3 Protein purification 12
2.1.4 DOTA-conjugation of $(HE)_3$-tagged proteins 13
2.2 Protein characterisation 14
2.2.1 Molecular weight analysis 14
2.2.2 Secondary structure and thermal stability evaluation 14
2.2.3 Target binding analysis 14
3 RESULTS 16
3.1 Protein production and ADAPT6 candidate selection 16
3.2 Protein characterisation and DOTA-conjugation 18
4 DISCUSSION AND CONCLUSIONS 23
5 ACKNOWLEDGEMENTS 25
6 REFERENCES 26
7 Appendix A 29

LIST OF ABBREVIATIONS AND ACRONYMS

$(HE)_3$	Histidine-glutamate-histidine-glutamate-histidine-glutamate
ABD	Albumin binding domain
ADAPT	ABD-derived affinity protein
CD	Circular dichroism
DTT	DL-Dithiothreitol
H_6	Hexahistidine
HER2	Human epidermal growth factor receptor 2
IEC	Ion exchange chromatography
IMAC	Immobilized metal ion affinity chromatography
MS	Mass spectrometry
ON	Overnight
PCR	Polymerase chain reaction
RP-HPLC	Reversed-phase high-performance liquid chromatography
SDS-PAGE	Sodium dodecyl sulfate-polyacrylamide gel electrophoresis
SPR	Surface plasmon resonance
TSB	Tryptic soy broth
VTM	Variable temperature measurement

1 INTRODUCTION

Cancer is a major cause of death worldwide and the annual cases are expecting to rise (1). The increasing cancer cases is a result of the growth and aging of the world population, but also the fact that people in economically developing countries are altering their lifestyles to more cancer-associated ones that includes smoking, lack of physical activity and unhealthy dietary choices (2).

Cancer treatment using targeted therapy involves the identification of and interference with therapeutic targets. The advantage with this type of therapy is that it aims to stop the growth and spreading of the cancerous cells while avoiding negative effects on healthy cells. One approach to identify patients who would benefit from a specific targeted therapy is to visualise the expression levels of the therapeutic target *in vivo* by radionuclide imaging (3).

One method of visualising diagnostic markers is to utilise molecular imaging together with protein-based imaging agents. An elevated level of a certain diagnostic marker on a tumour, for instance a growth receptor, can indicate the presence of cancer. Several different diagnostic markers, indicating different types of cancers, have been identified. However, diagnostic markers are often also expressed by healthy cells, although in lower levels. This can create problems if the diagnostic marker is also used in treatment to target the cancerous cells, since the treatment would also affect healthy cells. Sometimes expression of markers increases without cancer causing it. Also, not all patients with a specific cancer will have an increased expression of the marker.

1.1 Background

1.1.1 Albumin binding domain and ADAPT

The albumin binding domain (ABD) is a protein domain, with the ability to bind albumin, present in various surface proteins of several gram-positive bacteria (4). One of the ABDs of streptococcal protein G consists of 46 amino acids (5) and possesses a three helical structure with characteristics including high stability with respect to temperature and pH (6), high solubility and refold ability after thermal or chemical denaturation (5). Additionally, ABD has been used as a scaffold to develop new high-affinity binders to different targets by altering the amino acid composition on the surface while leaving the robust scaffold properties untouched (5,7).

One class of engineered affinity proteins that has been developed based on this scaffold is ABD-Derived Affinity ProTeins (ADAPTs) (5,7–9). ADAPT has the beneficial characteristics of ABD and the ability to bind new targets via altered amino acids on the surface. The altered amino acids are located away from the albumin binding site, enabling ADAPT to have bispecific properties (9).

1.1.2 Human epidermal growth factor receptor 2 and ADAPT6

The transmembrane protein human epidermal growth factor receptor 2 (HER2) is a tyrosine kinase receptor overexpressed in several cancer types. In healthy cells the expression is very low, making HER2 a suitable marker for the detection of cancer. Overexpression of HER2 occurs in 20-30 % of breast cancer tumours and is associated with disease reoccurrence and decreased survival (10). Moreover, several breast cancer therapies are targeting HER2 (11) and the selection of anti-HER2 therapy is performed by firstly detect HER2 expression in tumours (12).

ADAPT variants targeting HER2 have previously been developed (13) and one variant, called ADAPT6, has proven to be a suitable candidate for studying the visualisation of HER2-expressing tumours using molecular imaging. By alteration of amino acids on the surface, ADAPT6 has been engineered to bind HER2 with high affinity. Additionally, for ADAPT6 to bind specifically to HER2 the ability of binding albumin has been removed. Furthermore, ADAPT6 binds to the same epitope as trastuzumab (7), an anti-HER2 antibody that has been successful in both diagnostics and treatment of HER2-positive cancers. ADAPT6 is therefore a promising candidate for this application.

1.1.3 Molecular imaging

Molecular imaging is a non-invasive, repeatable approach to visualize tumours *in vivo* using a detectable imaging agent targeting disease associated markers. To receive high contrast images, an imaging agent is required to have high sensitivity and selectivity in order to accumulate in tumours while clearing quickly from blood and normal tissues. There are different molecular imaging techniques available, with single photon emission computed tomography (SPECT) imaging and positron emission tomography (PET) imaging being the main radionuclide-based ones, where for instance the radionuclides ^{111}In and ^{68}Ga respectively can be utilised.

Radiolabelled monoclonal antibodies have been utilised for imaging applications (14,15). However, due to limited penetration into tumours combined with slow blood and tissue clearance (16), antibodies often cause low imaging contrast. The imaging contrast has shown to be enhanced when using antibody fragments, due to that the smaller size allows faster clearance, which improves tumour-to-organ ratios (3). The smallest immunoglobulin-based imaging agents have the size of approximately 15 kDa (17). ADAPT is even smaller (~ 5 kDa), which makes it a promising candidate as an imaging agent. However, binding to albumin would result in slow blood clearance, considering that albumin is the most abundant protein in blood. The ability to bind albumin must therefore be eliminated to get high imaging contrasts. It has been shown that high contrast images can be obtained when using the HER2-binding ADAPT variant ADAPT6, which lack the ability of binding albumin, labelled with ^{111}In and ^{68}Ga (7).

For many cancers the liver is a main metastatic site, which is why unspecific uptake of the imaging agent in the liver is problematic. It has been studied how the composition of different histidine containing tags influences the biodistribution of another scaffold protein (18). It was found that positive charge and lipophilicity was correlated to a higher liver uptake. Of the tags that were studied, the lowest nonspecific uptake was achieved when a $(HE)_3$-tag was placed in

the N-terminus. The addition of a histidine-containing tag to a protein enables efficient purification using immobilized metal ion affinity chromatography (IMAC). Furthermore, the composition of the tag can affect the biodistribution of small proteins differently and earlier studies, with another small scaffold protein, have shown a more preferable biodistribution when a histidine-glutamate-histidine-glutamate-histidine-glutamate ($(HE)_3$-tag) has been utilised compared to a hexahistidine tag (H_6-tag) (19–22). However, when ADAPT6 was tested with either a $(HE)_3$-tag or a H_6-tag the uptake in normal organs was low for both variants (23). None of the tags gave a more preferable biodistribution which indicates that the effect of the tag varies between different engineered scaffold proteins and is dependent of the characteristics of the specific scaffold. A removal of the purification tag might also affect biodistribution and has earlier shown to result in lower hepatic uptake for another scaffold protein (20,21).

1.2 Aims and objectives

There is an interest to investigate whether it is possible to improve ADAPT6 as an imaging agent by increasing the tumour-to-organ radioactivity concentration ratios. Considering that the position of the radiolabel can contribute to off-target interactions which affect the biodistribution, a comparison of C-terminal labelled variants to already studied N-terminus labelled variants is desired. The aim of this degree project was to produce and characterise C-terminus altered ADAPT6 variants to enable the selection and production of most promising variants for later *in vivo* studies. The altered C-termini, containing an incorporated unique cysteine used for conjugation of a chelator, will be used for later radiolabelling prior to *in vivo* studies. The aim was to select ADAPT6 variants to be tested *in vivo* both with and without a purification tag in the N-terminus.

Characterisation included the evaluation of secondary structure and stability and also measurements of the target affinity.

To enable radiolabelling of ADAPT6, 1,4,7,10-tetraazacyclododecane-1,4,7-tris-acetic acid-10-maleimidoethylacetamide (maleimido-mono-amide-DOTA) was utilised. This is a maleimide derivative of the chelator DOTA which possesses the ability to bind radionuclides and was coupled covalently to ADAPT6 via a uniquely incorporated cysteine in the C-terminus. The ADAPT6 sequence itself contains no cysteines and therefore the incorporation of a cysteine gives a unique site for the chelator to bind.

2 MATERIAL AND METHODS

2.1 Protein production

2.1.1 Cloning

The ADAPT6 gene was amplified, from a cloning vector (pSCABD1) by polymerase chain reaction (PCR) using Q5 High-Fidelity DNA polymerase (New England Biolabs). The primers used (Table A1 and A2 in Appendix A) were designed to incorporate restriction sites and additional codons at the termini. In the C-terminus a unique cysteine was introduced to enable site-specific conjugation and in the N-terminus either the sequence MGHEHEHEDANS or MVDANS was introduced.

The amplified fragments were cleaved by the restriction enzymes NcoI and AscI and ligated into an expression vector that contained a kanamycin resistance gene for selection and a T7 promoter, upstream of the cleaving site, for induction of the incorporated gene. The vector was thereafter transformed into chemically competent *Escherichia coli (E. coli*) Top10 cells. Colonies were screened by PCR and sequences were analysed by Sanger sequencing. Colonies with correct incorporated fragments into the vector were cultured overnight (ON) and plasmids were received using QIAprep Spin Miniprep Kit (Qiagen). To confirm correct plasmids, the incorporated fragments were amplified using PCR. The PCR products were analysed on a 1 % agarose gel. Thereafter, plasmids were transformed into chemically competent *E. coli* BL21 cells for protein production.

2.1.2 Protein production

Proteins were produced by inoculating Tryptic soy broth (TSB) medium containing 50 µg/mL kanamycin with colonies carrying genes for the different ADAPT6 variants. The precultures were incubated at 37°C, 150 rpm ON and used for inoculation of TSB + yeast extract (TSB+Y) medium containing 50 µg/mL kanamycin. The amount of preculture used for inoculation was 1 % of the TSB+Y medium volume. The cultures were incubated at 37°C, 150 rpm and at $OD_{600} \approx 0.5\text{-}1.0$ were induced with 1 mM isopropyl β-D-1-thiogalactopyranoside (IPTG) and incubated at 25°C, 150 rpm ON for expression of the ADAPT6 variants. Harvest of the cells was performed by centrifugation at 2700 x g, 15 min, 4°C and the cells were resuspended in running buffer (50 mM NaP, 300 mM NaCl, pH 7.4 for the $(HE)_3$-tagged variants and 20 mM 2-(N-morpholino)ethanesulfonic acid (MES), pH 5.5 for the non-tagged variants). The cells were lysed by sonication (Vibra-Cell, Sonics & materials inc. Newtown, CT, USA) and cell debris was removed by centrifugation at 10 000 x g, 20 min, 4°C.

2.1.3 Protein purification

The characteristics of ADAPT6 in terms of high stability and ability of refolding after thermal denaturation, enabled heat treatment (90°C, 10 min) of the supernatants as a first purification step. The endogenous *E. coli* proteins that precipitated at 90°C were removed by centrifugation at 10 000 x g, 4°C, 20 min, and the supernatant was filtered through a 0.45 µm

filter. To examine the expression levels of the proteins, the supernatants (non-heat treated and heat treated) together with a cell sample taken before harvest, were analysed by sodium dodecyl sulfate-polyacrylamide gel electrophoresis (SDS-PAGE). Heat treated supernatants containing $(HE)_3$-tagged proteins were further purified by IMAC using Ni Sepharose™ 6 Fast Flow (GE Healthcare) as chromatography medium. For the equilibration, sample loading and washing steps a running buffer consisting of 50 mM NaP, 300 mM NaCl, pH 7.4, was used. Elution was performed by using a 0-150 mM imidazole gradient and fractions of 0.5 mL were collected.

The non-tagged variants were purified by ion exchange chromatography (IEC) using a 1 mL prepacked cation exchange column (RESOURCE S, GE Healthcare). Running buffer (20 mM MES, pH 5.5) was used for equilibration, sample loading and washing steps. Elution was performed by using a 0-1 M NaCl gradient and fractions were collected in 0.5 mL.

Fractions showing the highest absorbance at 280 nm were pooled together and the buffer was exchanged to 5 mM NH_4Ac pH 7.4 using PD-10 columns (GE Healthcare). Thereafter, the protein was freeze dried and resuspended in phosphate-buffered saline (PBS) buffer (150 mM NaCl, 8 mM Na_2HPO_4, 2 mM NaH_2PO_4), pH 7.4. Purified proteins were analysed by SDS-PAGE. The variant that was selected for *in vivo* studies was also analysed by reversed-phase high-performance liquid chromatography (RP-HPLC), to analyse the purity before DOTA-conjugation, using an analytical column (Zorbax 300 SB-C18 4.6 x 150 mm, 3.5 µm particle size, Agilent). Sample was loaded using 80% A, 20 % B (A: 0.1 % trifluoroacetic acid (TFA) in water, B: 0.1 % TFA in acetonitrile (ACN)). For the elution step, a 32-42 % gradient of buffer B over 30 min with a flow rate of 1 mL/min was applied.

2.1.4 DOTA-conjugation of $(HE)_3$-tagged proteins

DOTA-conjugation was performed on four $(HE)_3$-tagged variants prior to RP-HPLC purification. The chelator used in this project has a maleimide group attached, which enables conjugation since it binds the thiol group of the C-terminal cysteine. Before conjugation, proteins were reduced in PBS buffer, pH 7.4, by adding 20 mM DL-Dithiothreitol (DTT). The samples were incubated at 40°C for 30 min. To remove DTT after reduction, NAP-5 columns (GE Healthcare) were used with 5mM NH_4Ac, pH 7.4, with added Chelex (Bio-Rad) as the elution buffer. A 3 x molar excess of maleimido-mono-amide-DOTA chelator (Macrocyclics) was added to the reduced proteins followed by incubation at 40°C, 1 h. Thereafter, a freeze drying step was performed to later resuspend the proteins in 80% A, 20 % B (A: 0.1 % TFA in water, B: 0.1 % TFA in ACN).

RP-HPLC was utilised to purify the proteins from excess chelators and also to remove any remaining impurities. Depending on the volume of the samples, a semipreparative column (Zorbax 300 SB-C18 9.4 x 250 mm, 5 µm particle size, Agilent) or an analytical column (Zorbax 300 SB-C18 4.6 x 150 mm, 3.5 µm particle size, Agilent) was used. Sample was loaded using 80 % A, 20 % B (A: 0.1 % TFA in water, B: 0.1 % TFA in ACN). For the elution step, a 35-36.5 % gradient of buffer B over 30 min with the flow rate 3 mL/min was applied when using the semipreparative column. In the elution step when the analytical column was used, the gradient of buffer B was 32-42 % over 30 min with the flow rate 1 mL/min. Purified proteins were analysed by MS, freeze dried and later resuspended in 5 mM NH_4Ac pH 7.4 with added Chelex (Bio-Rad).

The purity of the DOTA-conjugated $(HE)_3$-tagged variant that was selected for *in vivo* studies was analysed by SDS-PAGE and by RP-HPLC using an analytical column (Zorbax 300 SB-C18 4.6 x 150 mm, 3.5 µm particle size, Agilent). Sample was loaded using 80 % A, 20 % B (A: 0.1 % TFA in water, B: 0.1 % TFA in ACN). The protein was eluted by applying a 25-50 % gradient of buffer B over 30 min with a flow rate of 1 mL/min. Data received from all RP-HPLC experiments was plotted and analysed using Agilent ChemStation (version B.04.01, Agilent Technologies, Santa Clara California USA).

2.2 Protein characterisation

2.2.1 Molecular weight analysis

Mass spectrometry (MS) was utilised to analyse the molecular weight of the ADAPT6 variants produced. The method used was time-of-flight MS using a 4800 MALDI TOF/TOF Analyzer (MDS SCIEX, Toronto, Canada), where alpha-cyano-4-hydroxycinnamic acid was used as matrix. Data was exported from 4000 Series Explore software (Version 3.7, AB SCIEX) to Data Explorer software (AB SCIEX) to receive MS spectra.

2.2.2 Secondary structure and thermal stability evaluation

To evaluate the secondary structure of the ADAPT6 candidates, circular dichroism (CD) spectroscopy was utilised, using a JASCO J-810 spectropolarimeter (JASCO, Tokyo, Japan). The samples analysed were diluted in PBS buffer, pH 7.4, to concentrations of 0.4-0.5 mg/mL and by measuring the degree of ellipticity at wavelengths from 250 to 195 nm at 25°C, the secondary structure could be evaluated. Measurements were taken five times to receive an average plot. To evaluate whether heat affects the secondary structure, this measurement was performed before and after a thermal stability measurement, called variable temperature measurement (VTM), where ellipticity was measured at 221 nm at temperatures ranging from 20 to 90°C. The plotted values from the thermal stability measurement were used to fit a Boltzmann sigmoidal curve, which was used to estimate melting temperatures. Data from CD measurements and VTM was plotted and analysed using GraphPad Prism (version 7.01 for Windows, GraphPad Software, San Diego California USA).

2.2.3 Target binding analysis

For the evaluation of the binding to the target HER2, surface plasmon resonance (SPR) was performed using a Biacore T200 (GE Healthcare Bio-Sciences AB, Uppsala, Sweden). The sensor chip used for this experiment was a CM5 sensor chip immobilized with human recombinant HER2 (Sino biological), on two surfaces, to the levels of 550 and 1000 response units (RU) respectively.

10 mM HCl was used as regeneration solution to regenerate the surfaces after each measurement. A flow rate of 30 µL/min was used for all analyses, using PBS buffer supplemented with 0.05 % Tween 20 (PBST), pH 7.4, as running buffer. The association and dissociation times were set to 500 s and 1000 s respectively. A 1:2 dilution series was

prepared for the analytes to obtain five concentrations, from 50 nM to 3.125 nM in PBST, pH 7.4. To receive binding affinity information, dissociation constants (K_D) were estimated by fitting the received data to a 1:1 Langmuir binding isotherm using Biacore T200 Evaluation Software (version 2.0, General Electric Company, Fairfield Connecticut USA).

3 RESULTS

3.1 Protein production and ADAPT6 candidate selection

Nine $(HE)_3$-tagged ADAPT6 variants with different C-termini were cloned to examine which variants that were able to be expressed highly enough, with the reasoning of preferring the shortest variant possible. The composition of the different amino acid sequences in the C-termini is shown in Table A2 in Appendix A. All nine candidates were successfully expressed in *E. coli*, leading to the decision to continue with the four shorter variants G-$(HE)_3$-DANS-ADAPT6-C, G-$(HE)_3$-DANS-ADAPT6-GC, G-$(HE)_3$-DANS-ADAPT6-GSC, G-$(HE)_3$-DANS-ADAPT6-GSSC. The four variants were purified by heat treatment and IMAC, freeze dried, resuspended in PBS buffer, pH 7.4, and thereafter analysed by SDS-PAGE, MS and CD. Samples with the two variants G-$(HE)_3$-DANS-ADAPT6-C (~ 6 kDa) and G-$(HE)_3$-DANS-ADAPT6-GSSC (~ 7 kDa) were loaded on the same SDS-PAGE gel, showing high expression of both variants (Figure 1). The gel also shows that the IMAC purification of G-$(HE)_3$-DANS-ADAPT6-C was successful with almost no protein in the flow-through. Two eluted fractions, B3 and B8 were loaded on the gel and both showed a band at the expected weight. The molecular weights were confirmed by MS and CD measurements showed that the variants all had a clear alpha helix secondary structure and melting temperatures between 60-67°C. Furthermore, all variants retained the alpha helix structure after the thermal stability measurement. Therefore, all four $(HE)_3$-tagged variants were DOTA-conjugated and the analysis by RP-HPLC and MS confirmed that the DOTA-conjugation was successful.

The fact that all four variants showed positive results with respect to production and characterisation, it was decided that the shortest variant, G-$(HE)_3$-DANS-ADAPT6-C, should be tested *in vivo* together with a corresponding non-tagged variant. Four variants, with different C-terminal sequences, were cloned without the $(HE)_3$-tag for an expression analysis. The expression analysis showed that all non-tagged variants (~ 6 kDa) had low expression levels and no expression for the desired shortest variant MVDANS-ADAPT6-C (Figure 2), which was the corresponding non-tagged variant to the chosen $(HE)_3$-tagged variant G-$(HE)_3$-DANS-ADAPT6-C. The longest variant MVDANS-ADAPT6-GSSC showed the highest expression level. However, there was expression of the second shortest variant, MVDANS-ADAPT6-GC, even if it was noticeably lower than for the longest variant.

Therefore, the variants MVDANS-ADAPT6-GC and MVDANS-ADAPT6-GSSC were produced and purified using heat treatment followed by IEC. The eluted fractions had very low absorbance at 280 nm for both variants and samples from the different steps of the production and purification of MVDANS-ADAPT6-GC were analysed by SDS-PAGE. The gel showed that the protein (~ 6 kDa) was present in eluted fractions (Figure 3). SDS-PAGE analysis of MVDANS-ADAPT6-GSSC showed low expression for the variant compared to the $(HE)_3$-tagged variants (Figure 1). Additionally, the gels demonstrate that several unwanted proteins were removed during the heat treatment, without significantly loss of the target protein. However, within the time frame of this work it was not possible to produce enough of the non-tagged variants for the following experiments.

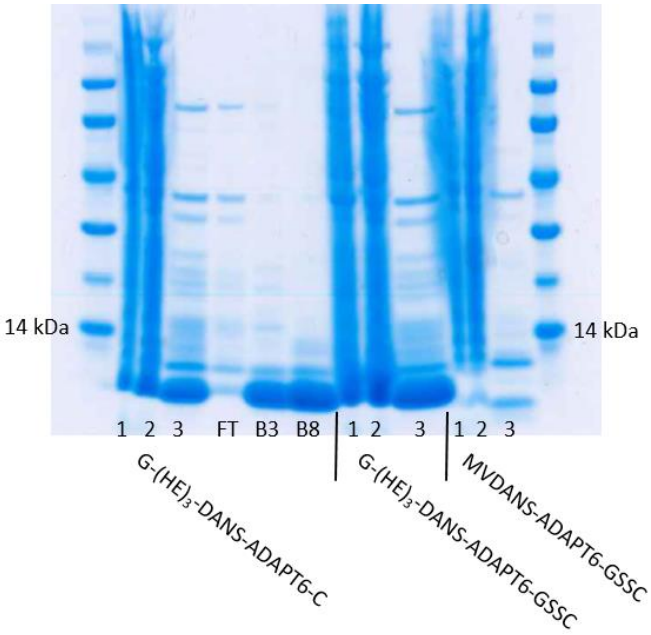

Figure 1. SDS-PAGE analysis of G-(HE)$_3$-DANS-ADAPT6-C, G-(HE)$_3$-DANS-ADAPT6-GSSC and MVDANS-ADAPT6-GSSC. Ladder: LMW-SDS Marker Kit (GE Healthcare). 1: pellet sample (culture sample taken before harvest and pellet received after centrifugation at 17 900 x g, 10 min). 2: supernatant before heat treatment. 3: supernatant after heat treatment. FT: Flow-through from IMAC purification. B3 and B8: two different eluted fractions from IMAC purification.

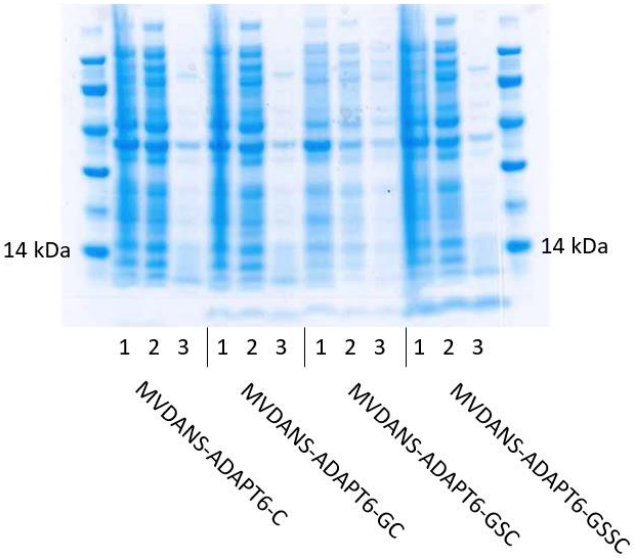

Figure 2. SDS-PAGE analysis of MVDANS-ADAPT6-C, MVDANS-ADAPT6-GC, MVDANS-ADAPT6-GSC and MVDANS-ADAPT6-GSSC. Ladder: LMW-SDS Marker Kit (GE Healthcare). 1: pellet sample (culture sample taken before harvest and pellet received after centrifugation at 17 900 x g, 10 min). 2: supernatant before heat treatment. 3: supernatant after heat treatment.

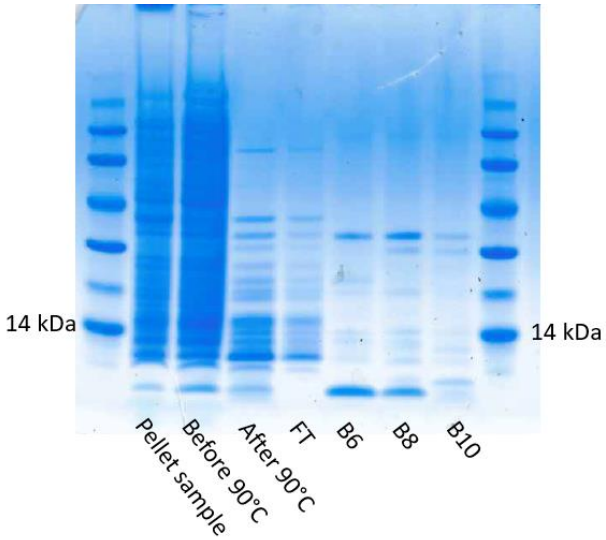

Figure 3. SDS-PAGE analysis of MVDANS-ADAPT6-GC before and after IEC purification. Ladder: LMW-SDS Marker Kit (GE Healthcare). Pellet sample: culture sample taken before harvest and pellet received after centrifugation at 17 900 x g, 10 min. Before 90°C: supernatant before heat treatment. After 90°C: supernatant after heat treatment. FT: flow-through. B6, B8, B10: different eluted fractions.

3.2 Protein characterisation and DOTA-conjugation

DOTA-conjugation was performed, for the four $(HE)_3$-tagged variants, followed by freeze drying and resuspension in RP-HPLC running buffer prior to RP-HPLC purification. MS was performed after the purification and confirmed that the DOTA-conjugation was successful for all variants. The shortest variant G-$(HE)_3$-DANS-ADAPT6-C was chosen for *in vivo* studies. Prior to the DOTA-conjugation of this variant, RP-HPLC was performed to analyse the purity of the sample. Freeze dried G-$(HE)_3$-DANS-ADAPT6-C was resuspended in PBS buffer, pH 7.4, and reduced in 20 mM DTT to break any disulphide bridges before RP-HPLC. This variant was shown to have a purity of 94 % prior to DOTA-conjugation. In addition to MS, SDS-PAGE was also performed to confirm that the DOTA-conjugation of this variant was successful (Figure 4). The DOTA-conjugation provides the protein with ~526 Da extra of weight, resulting in a band higher up on the SDS-PAGE gel indicating a higher molecular weight. The difference is small, but noticeable. However, MS also indicated the presence of non-conjugated protein after purification. It is known that the initial methionine in proteins often is removed (24–31). Therefore, the measured weights were compared to theoretical weights of the ADAPT6 variants with and without the initial methionine. The molecular weights detected indicated that the initial methionine of the $(HE)_3$-tagged variants, but not the non-tagged variants, was cleaved off. The theoretical molecular weight of G-$(HE)_3$-DANS-ADAPT6-C is 6445.2 Da when non-conjugated and 6971.2 Da when DOTA-conjugated, which is in good agreement with the MS data in Figure 4 b (6440.2 Da and 6970.7 Da). It was therefore concluded that the variant produced for *in vivo* studies lacked the initial methionine. In total, approximately 18.9 mg of purified G-$(HE)_3$-DANS-ADAPT6-C was received from a 200 mL culture (94.6 mg/L) and of this 7.3 mg was DOTA-conjugated. After RP-HPLC purification, 2.2 mg G-$(HE)_3$-DANS-ADAPT6-C-DOTA was received (5.8 mg/L).

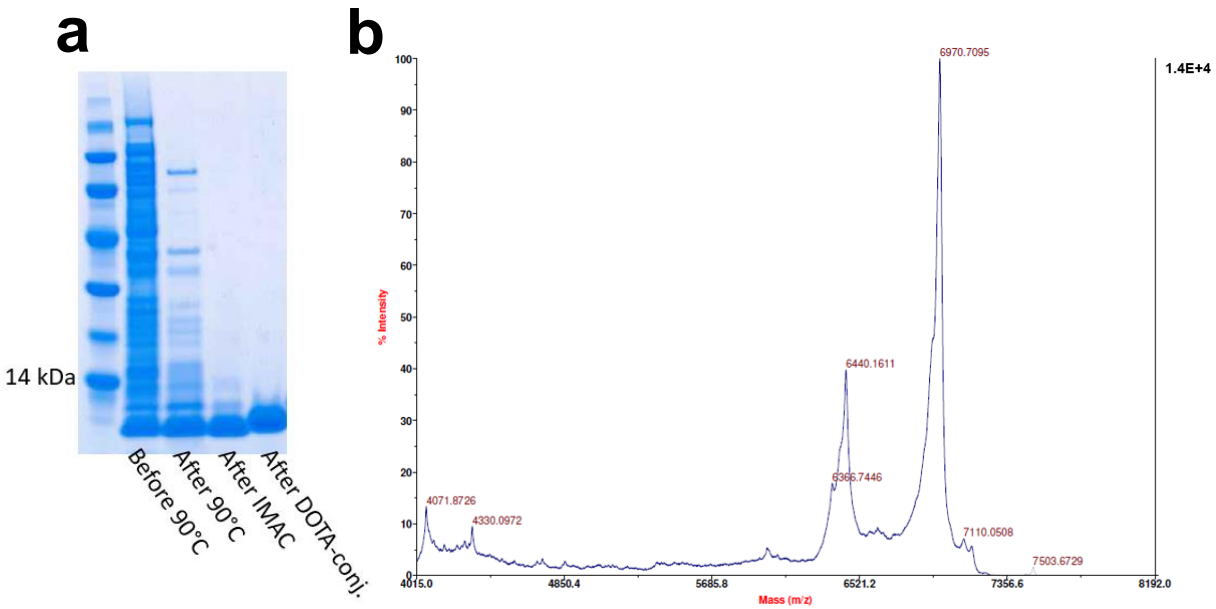

Figure 4. SDS-PAGE and MS analysis of G-(HE)$_3$-DANS-ADAPT6-C and G-(HE)$_3$-DANS-ADAPT6-C-DOTA.

a. SDS-PAGE analysis of G-(HE)$_3$-DANS-ADAPT6-C and G-(HE)$_3$-DANS-ADAPT6-C-DOTA. Ladder: LMW-SDS Marker Kit (GE Healthcare). Before 90°C: supernatant before heat treatment. After 90°C: supernatant after heat treatment. After IMAC: IMAC purified protein (non-conjugated). After DOTA-conj.: DOTA-conjugated protein after RP-HPLC purification.

b. MS spectrum of RP-HPLC purified G-(HE)$_3$-DANS-ADAPT6-C-DOTA. The spectrum shows two clear peaks at 6440.2 and 6970.7 Da.

The characteristic shape of an alpha helix curve was received from CD measurements for both G-(HE)$_3$-DANS-ADAPT6-C and G-(HE)$_3$-DANS-ADAPT6-C-DOTA, indicating a clear alpha helix secondary structure before and after VTM (Figure 5). Figure 6 is showing an example of a VTM curve, for G-(HE)$_3$-DANS-ADAPT6-C-DOTA, used for melting temperature estimation. The melting temperatures were estimated to be 63 and 59°C for the non-conjugated and conjugated protein respectively (Table 1). Although the chelator lowers the melting temperature to some degree, this ADAPT6 variant is stable and maintains the ability to refold after thermal denaturation.

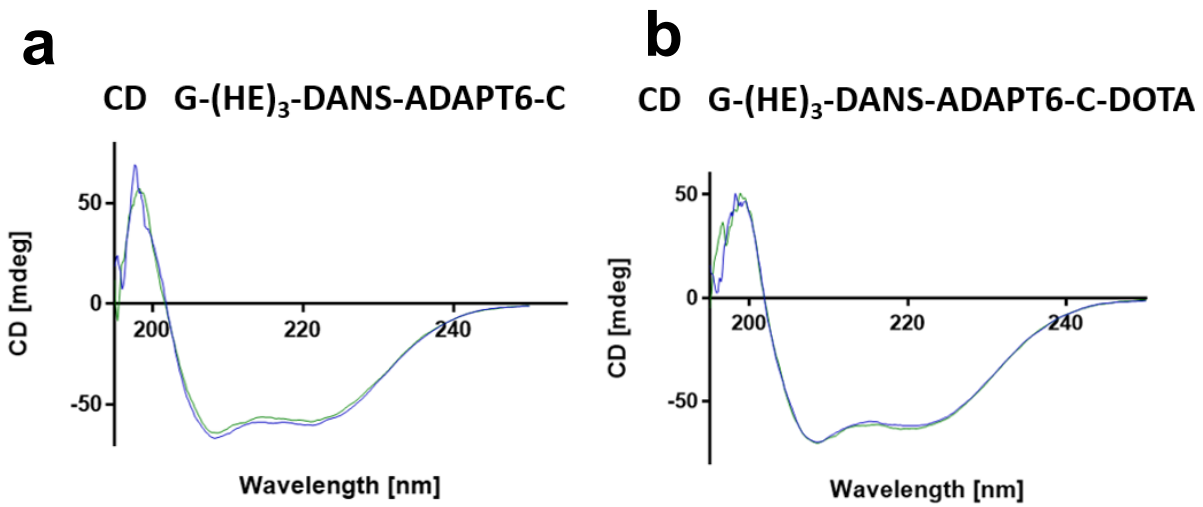

Figure 5. CD measurements of G-(HE)$_3$-DANS-ADAPT6-C and G-(HE)$_3$-DANS-ADAPT6-C-DOTA. The blue curve represents the CD measurement before the VTM and the green curve represents the CD measurement after the VTM.
a. Non-conjugated ADAPT6 candidate (G-(HE)$_3$-DANS-ADAPT6-C).
b. Conjugated ADAPT6 candidate (G-(HE)$_3$-DANS-ADAPT6-C-DOTA).

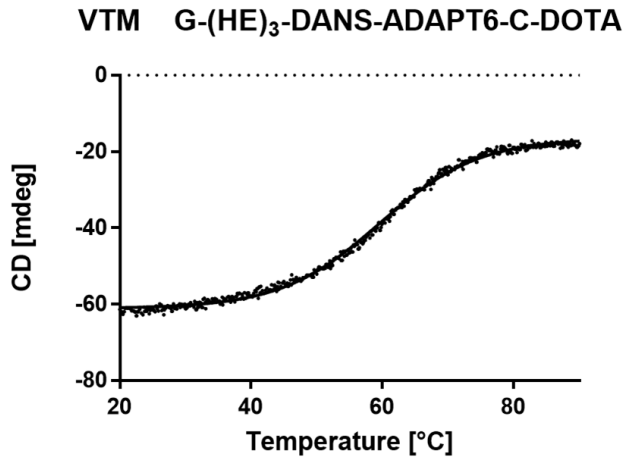

Figure 6. VTM of G-(HE)$_3$-DANS-ADAPT6-C-DOTA. Plotted data points together with a fitted Boltzmann sigmoidal curve, used for melting temperature estimation.

Table 1. Melting temperatures of G-(HE)$_3$-DANS-ADAPT6-C and G-(HE)$_3$-DANS-ADAPT6-C-DOTA.

	melting temperature, measurement 1 (°C)	melting temperature, measurement 2 (°C)	average melting temperature (°C)
G-(HE)$_3$-DANS-ADAPT6-C	64	61	63
G-(HE)$_3$-DANS-ADAPT6-C-DOTA	60	59	59

To determine the purity of the G-$(HE)_3$-DANS-ADAPT6-C-DOTA sample, RP-HPLC was performed (Figure 7) using the same sample as for the MS spectrum in Figure 4 b. One clear peak was detected, at the absorbance at 280 nm, representing a purity of 99 %. Although MS indicated that there was some non-conjugated protein left, it was not a significant amount according to the RP-HPLC analysis. It may be beneficial to use various analysis methods since different methods may display different results.

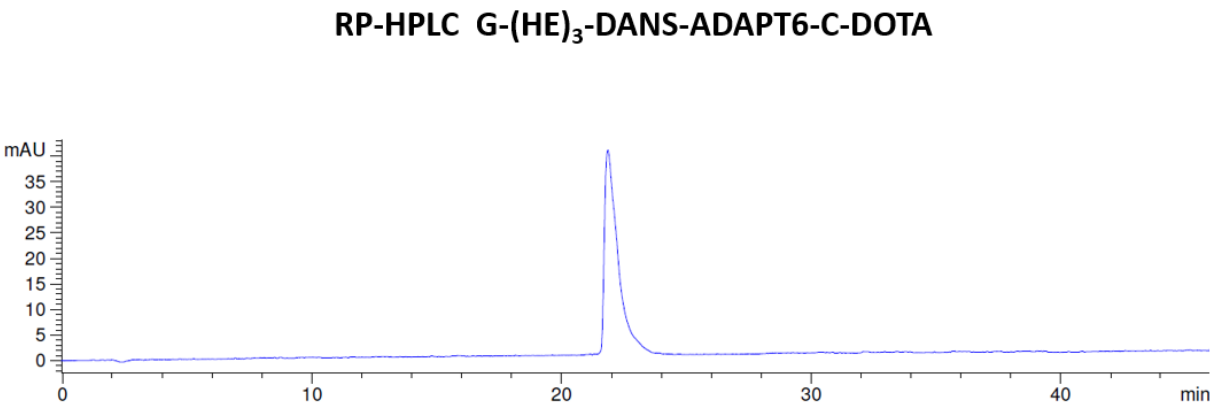

Figure 7. RP-HPLC chromatogram from purity analysis of G-$(HE)_3$-DANS-ADAPT6-C-DOTA. The y-axis is showing the absorbance at 280 nm in absorbance units (AU).

SPR was performed to confirm the binding to the target HER2 (Figure 8). G-$(HE)_3$-DANS-ADAPT6-C-DOTA showed affinity to HER2 in the nanomolar range. The binding capacity to the target was therefore not lost after incorporation of a new amino acid in the C-terminus along with conjugation of the DOTA chelator. K_D was estimated to be 2.5 nM. The fitted curve for the 50 nM sample was not fully aligned and was therefore removed to give a more accurate approximation of the K_D value. A summary of the characterisation is shown in Table 2.

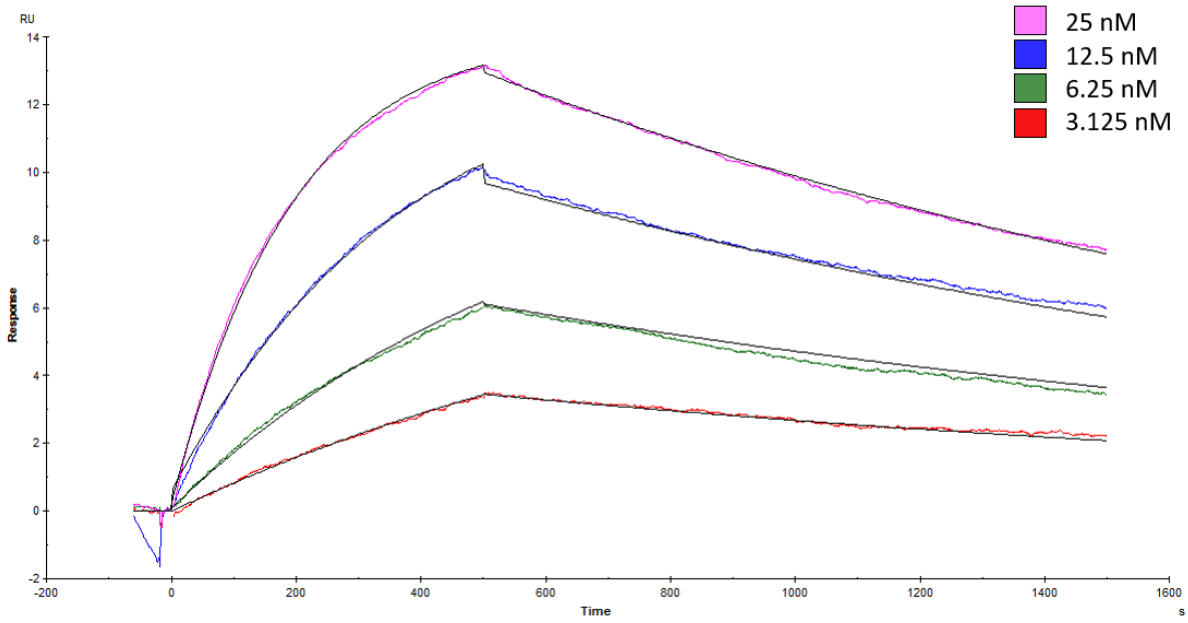

Figure 8. SPR measurement of G-(HE)$_3$-DANS-ADAPT6-C-DOTA. The different curves represent different ADAPT6 concentrations, indicated by the different colours. The black lines represent the fitted curves (1:1 Langmuir binding isotherm).

Table 2. Characterisation summary of G-(HE)$_3$-DANS-ADAPT6-C and G-(HE)$_3$-DANS-ADAPT6-C-DOTA.

	theoretical molecular weight (Da)	experimental molecular weight (Da)	melting temperature (°C)	purity (%)	K_D (nM)
G-(HE)$_3$-DANS-ADAPT6-C	6445.2	6439.8	63	94	-
G-(HE)$_3$-DANS-ADAPT6-C-DOTA	6971.2	6970.7	59	99	2.5

4 DISCUSSION AND CONCLUSIONS

The use of small affinity scaffold proteins engineered to target diagnostic markers appears like a promising approach in cancer diagnostics, where ADAPTs have many favourable characteristics including the ability to be engineered to bind different targets with high affinity, a small size, high stability and also refolding properties after denaturation. The ADAPT variant studied in this project, ADAPT6, has been designed to target the breast cancer associated receptor HER2 by altering amino acids on the surface and to lack the ability to bind albumin, through point mutations in the albumin binding interface. ADAPT6 has previously been tested as an imaging agent in *in vivo* imaging studies, visualising HER2 expressing tumours, where high contrast images could be obtained (7,23). In this project, new ADAPT6 variants with different terminal compositions were produced to be compared with already existing variants with the aim to examine whether this imaging agent can be improved further.

To enable radiolabelling, a maleimide derivative of the chelator DOTA was coupled covalently to ADAPT6 via a uniquely incorporated C-terminal cysteine. Considering that ADAPT6 has no other cysteines in its sequence, the incorporated cysteine provided a unique site for the chelator to bind. It is of importance to have a unique binding site for the chelator to obtain a site-specific labelled protein. In that way the position of the radiolabel is known and in this project the chelator was positioned away from the binding site to minimise the risk of influencing the binding to the target.

In this project, nine different $(HE)_3$-tagged ADAPT6 variants were cloned to first examine which ones that could be expressed. All the variants had a unique C-terminal cysteine and they differed by the addition of a few extra amino acids with varying composition, for details see Table A2 Appendix A. A few extra amino acids were introduced before the cysteine in the C-terminus in eight of the variants to allow more flexibility, since the third ADAPT6 helix ends with a rigid proline. However, the shortest variant which had the cysteine next to the proline could be expressed and DOTA-conjugated without losing the secondary structure or binding ability to HER2.

One of the purification methods to purify the $(HE)_3$-tagged variants was to use IMAC. It has been shown earlier that when purifying proteins by using a $(HE)_3$-tag, problem of binding to the resin can occur if imidazole, even in low concentrations, is included in the running buffer (23). This effect is not surprising considering a $(HE)_3$-tag has half the amount of histidines compared to a H_6-tag. Therefore, no imidazole was added to the running buffer.

The variant produced in this degree project appears to be a suitable imaging agent candidate for *in vivo* studies considering its small size, preserved stability, HER2 binding ability and the fact that ADAPT6 has been a successful imaging agent in earlier *in vivo* studies (7,23). Considering that the ability to bind HER2 remained when tested *in vitro*, G-$(HE)_3$-DANS-ADAPT6-C-DOTA can most likely bind to tumour cells expressing HER2 *in vivo*. It remains to be seen whether this variant has an improved biodistribution profile compared to previously studied N-terminal labelled variants. However, the selected variant was difficult to express without the purification tag. When the amino acid sequence MG-$(HE)_3$-DANS was changed to MVDANS in the N-terminus, expression problems occurred. For all the $(HE)_3$-tagged

variants high expression was observed, while the expression of the non-tagged variants was very low. Optimisation of the termini in the non-tagged variants is necessary, to enable production and characterisation, before *in vivo* studies can be performed. Cloning and expression analysis of five new, non-tagged ADAPT6 variants, with different N-termini, has already been initiated in the hope of finding a variant that can easily be produced. It is not known if it is the composition of the N-terminus that is the problem, but it has been observed that expression problems occur when the sequence in the N-terminus is shortened.

Considering that mice will be used in the *in vivo* studies it is of great importance to carefully assess ethical aspects and avoid examining poor candidates or performing experiments that are unnecessary. Before the *in vivo* studies it is important to firstly have a pure imaging agent. Also, further experiments will be performed before introducing the imaging agent intravenously into living mice. Experiments to be performed include radiolabelling, followed by purification and label stability measurements to ensure that no radionuclide is released from the conjugate. An *in vitro* cell binding experiment will be performed where the binding affinity, of the radiolabelled variant, to HER2-expressing cancerous cells will be measured. Furthermore, the future *in vivo* studies will be performed in accordance with national legislation on laboratory animals' protection and must be approved by the Ethics Committee for Animal Research in Uppsala. The *in vivo* studies will be performed in Uppsala by Vladimir Tolmachev's och Anna Orlova's groups.

For molecular imaging purposes it is important to eliminate the albumin binding ability of ADAPT as described earlier. However, if ADAPT would instead be used in targeted therapy, it would be of high interest to study whether increasing the half-life of ADAPT in the blood would allow a prolonged therapeutic effect. Considering the long half-life of albumin in the blood, it would be desired to retain the ability of binding albumin, with the aim to increase the half-life of ADAPT in the blood. Several studies have demonstrated that albumin binding provides the potential of obtaining longer half-lives of therapeutic proteins (32). For ADAPT to function as a therapeutic protein, new characteristics must be added since ADAPT itself does not stop the development of cancer. Another possibility might be to couple a drug, that inhibits both the growth and spreading of cancerous cells, to the ADAPT molecule.

5 ACKNOWLEDGEMENTS

First, I would like to thank my supervisor Sophia Hober and also Sarah Lindbo for all the guidance and support throughout this degree project. Also, I would like to thank Sarah Lindbo for the introduction to the laboratory and for instructing me when it was needed. To all at the department of protein technology at KTH, would I like to give thanks for the friendly reception and helpfulness in the laboratory. I would also like to thank my scientific reviewer Fredrik Frejd for helpful critical review of this work. Finally, I would like to thank Affibody AB for allowing me to perform CD measurements using their spectropolarimeter. I am very grateful for the opportunity I was given to work with this project. The experience has been both exciting and educational.

6 REFERENCES

1. Stewart BW, Wild C, International Agency for Research on Cancer, World Health Organization, editors. World cancer report 2014. Lyon, France: International Agency for Research on Cancer; 2014. 630 p.

2. Jemal A, Bray F, Center MM, Ferlay J, Ward E, Forman D. Global cancer statistics. CA Cancer J Clin. 2011 Mar;61(2):69–90.

3. Tolmachev V, Stone-Elander S, Orlova A. Radiolabelled receptor-tyrosine-kinase targeting drugs for patient stratification and monitoring of therapy response: prospects and pitfalls. Lancet Oncol. 2010 Oct;11(10):992–1000.

4. Navarre WW, Schneewind O. Surface Proteins of Gram-Positive Bacteria and Mechanisms of Their Targeting to the Cell Wall Envelope. Microbiol Mol Biol Rev. 1999 Mar;63(1):174–229.

5. Nilvebrant J, Hober S. The albumin-binding domain as a scaffold for protein engineering. Comput Struct Biotechnol J. 2013 Mar;6(7):1–8.

6. Johansson MU, de Château M, Björck L, Forsén S, Drakenberg T, Wikström M. The GA module, a mobile albumin-binding bacterial domain, adopts a three-helix-bundle structure. FEBS Lett. 1995 Sep 11;374:257–61.

7. Garousi J, Lindbo S, Nilvebrant J, Astrand M, Buijs J, Sandstrom M, et al. ADAPT, a Novel Scaffold Protein-Based Probe for Radionuclide Imaging of Molecular Targets That Are Expressed in Disseminated Cancers. Cancer Res. 2015 Oct 15;75(20):4364–71.

8. Nilvebrant J, Alm T, Hober S, Löfblom J. Engineering Bispecificity into a Single Albumin-Binding Domain. Hoheisel JD, editor. PLoS ONE. 2011 Oct 3;6(10):e25791.

9. Alm T, Yderland L, Nilvebrant J, Halldin A, Hober S. A small bispecific protein selected for orthogonal affinity purification. Biotechnol J. 2010 Jun;5(6):605–17.

10. Slamon DJ, Clark GM, Wong SG, Levin WJ, Ullrich A, McGuire WL. Human breast cancer: correlation of relapse and survival with amplification of the HER-2/neu oncogene. Science. 1987 Jan 9;235(4785):177–82.

11. Giordano SH, Temin S, Kirshner JJ, Chandarlapaty S, Crews JR, Davidson NE, et al. Systemic Therapy for Patients With Advanced Human Epidermal Growth Factor Receptor 2-Positive Breast Cancer: American Society of Clinical Oncology Clinical Practice Guideline. J Clin Oncol. 2014 Jul 1;32(19):2078–99.

12. Wolff AC, Hammond MEH, Hicks DG, Dowsett M, McShane LM, Allison KH, et al. Recommendations for Human Epidermal Growth Factor Receptor 2 Testing in Breast Cancer: American Society of Clinical Oncology/College of American Pathologists Clinical Practice Guideline Update. J Clin Oncol. 2013 Nov 1;31(31):3997–4013.

13. Nilvebrant J, Åstrand M, Georgieva-Kotseva M, Björnmalm M, Löfblom J, Hober S. Engineering of Bispecific Affinity Proteins with High Affinity for ERBB2 and Adaptable Binding to Albumin. Hoheisel JD, editor. PLoS ONE. 2014 Aug 4;9(8):e103094.

14. Dijkers EC, Oude Munnink TH, Kosterink JG, Brouwers AH, Jager PL, de Jong JR, et al. Biodistribution of 89Zr-trastuzumab and PET Imaging of HER2-Positive Lesions in Patients With Metastatic Breast Cancer. Clin Pharmacol Ther. 2010 May;87(5):586–92.

15. Gaykema SBM, Brouwers AH, Lub-de Hooge MN, Pleijhuis RG, Timmer-Bosscha H, Pot L, et al. 89Zr-Bevacizumab PET Imaging in Primary Breast Cancer. J Nucl Med. 2013 Jul 1;54(7):1014–8.

16. Jain RK. Physiological barriers to delivery of monoclonal antibodies and other macromolecules in tumors. Cancer Res. 1990 Feb 1;50(3 Suppl):814s–819s.

17. Chakravarty R, Goel S, Cai W. Nanobody: The 'Magic Bullet' for Molecular Imaging? Theranostics. 2014;4(4):386–98.

18. Hofström C, Altai M, Honarvar H, Strand J, Malmberg J, Hosseinimehr SJ, et al. HAHAHA, HEHEHE, HIHIHI, or HKHKHK: Influence of Position and Composition of Histidine Containing Tags on Biodistribution of $[\,^{99m}Tc(CO)_3\,]^+$ -Labeled Affibody Molecules. J Med Chem. 2013 Jun 27;56(12):4966–74.

19. Orlova A, Nilsson FY, Wikman M, Widström C, Ståhl S, Carlsson J, et al. Comparative in vivo evaluation of technetium and iodine labels on an anti-HER2 affibody for single-photon imaging of HER2 expression in tumors. J Nucl Med Off Publ Soc Nucl Med. 2006 Mar;47(3):512–9.

20. Ahlgren S, Wallberg H, Tran TA, Widstrom C, Hjertman M, Abrahmsen L, et al. Targeting of HER2-Expressing Tumors with a Site-Specifically 99mTc-Labeled Recombinant Affibody Molecule, ZHER2:2395, with C-Terminally Engineered Cysteine. J Nucl Med. 2009 May 1;50(5):781–9.

21. Ahlgren S, Orlova A, Rosik D, Sandström M, Sjöberg A, Baastrup B, et al. Evaluation of Maleimide Derivative of DOTA for Site-Specific Labeling of Recombinant Affibody Molecules. Bioconjug Chem. 2008 Jan;19(1):235–43.

22. Tolmachev V, Hofström C, Malmberg J, Ahlgren S, Hosseinimehr SJ, Sandström M, et al. HEHEHE-Tagged Affibody Molecule May Be Purified by IMAC, Is Conveniently Labeled with $[\,^{99m}Tc(CO)_3\,]^+$, and Shows Improved Biodistribution with Reduced Hepatic Radioactivity Accumulation. Bioconjug Chem. 2010 Nov 17;21(11):2013–22.

23. Lindbo S, Garousi J, Åstrand M, Honarvar H, Orlova A, Hober S, et al. Influence of Histidine-Containing Tags on the Biodistribution of ADAPT Scaffold Proteins. Bioconjug Chem. 2016 Mar 16;27(3):716–26.

24. Capecchi MR. Initiation of E. coli proteins. Proc Natl Acad Sci. 1966 Jun 1;55(6):1517–24.

25. Adams JM. On the Release of the Formyl Group from Nascent Protein. J Mol Biol. 1968 May 14;33(3):571–89.

26. Takeda M, Webster RE. Protein chain initiation and deformylation in B. subtilis homogenates. Proc Natl Acad Sci. 1968 Aug 1;60(4):1487–94.

27. Pine MJ. Kinetics of maturation of the amino termini of the cell proteins of Escherichia coli. Biochim Biophys Acta BBA - Nucleic Acids Protein Synth. 1969 Jan;174(1):359–72.

28. Yoshida A, Lin M. NH2-Terminal Formylmethionine- and NH2-Terminal Methionine Cleaving Enzymes in Rabbits. J Biol Chem. 1972 Feb 10;247(3):952–7.

29. Housman D, Gillespie D, Lodish HF. Removal of formyl-methionine residue from nascent bacteriophage f2 protein. J Mol Biol. 1972 Mar;65(1):163–6.

30. Ball LA, Kaesberg P. Cleavage of the N-terminal Formymlethionine Residue from a Bacteriophage Coat Protein in vitro. J Mol Biol. 1973 Sep 25;79(3):437–598.

31. Tsunasawa S, Stewart JW, Sherman F. Amino-terminal Processing of Mutant Forms of Yeast Iso-1-cytochrome c. J Biol Chem. 1985 May 10;260(9):5382–91.

32. Kontermann RE. Strategies for extended serum half-life of protein therapeutics. Curr Opin Biotechnol. 2011 Dec;22(6):868–76.

7 Appendix A

Table A1. Forward primers.

	Primer	Translates to
Variants with $(HE)_3$-tag:	AAAACCATGGGCCATGAGCATGAGCATGAGGACGCGAATAGCTTAGCT	KT Met GHEHEHEDANSLA
Variants without $(HE)_3$-tag (MVDANS):	AAAACCATGGTCGACGCGAATTCATTAGCT	KT Met VDANSLA

Table A2. Reverse primers. Amino acids added in the C-terminus are marked with green colour.

	Primer	Translates to
MG-$(HE)_3$-DANS-ADAPT6-C or MVDANS-ADAPT6-C:	TGTTGTCTACGGGCGCGCCTTAACAGGGTAATGC	ALP**C** Stop GAPVDN
MG-$(HE)_3$-DANS-ADAPT6-GC or MVDANS-ADAPT6-GC:	TTTTTTGGCGCGCCTTAACAGCCGGGTAATGCATGTAAAATTTC	EILHALP**GC** Stop GAPK
MG-$(HE)_3$-DANS-ADAPT6-GGC or MVDANS-ADAPT6-GGC:	TTTTTTGGCGCGCCTTAACAGCCACCGGGTAATGCATGTAAAATTTC	EILHALP**GGC** Stop GAPK
MG-$(HE)_3$-DANS-ADAPT6-GGGC or MVDANS-ADAPT6-GGGC:	TTTTTTGGCGCGCCTTAACAGCCACCGCCGGGTAATGCATGTAAAATTTC	EILHALP**GGGC** Stop GAPK
MG-$(HE)_3$-DANS-ADAPT6-GGGGC or MVDANS-ADAPT6-GGGGC:	TTTTTTGGCGCGCCTTAACAGCCACCGCCACCGGGTAATGCATGTAAAATTTC	EILHALP**GGGGC** Stop GAPK
MG-$(HE)_3$-DANS-ADAPT6-GSC or MVDANS-ADAPT6-GSC:	TTTTTTGGCGCGCCTTAACAGCTACCGGGTAATGCATGTAAAATTTC	EILHALP**GSC** Stop GAPK
MG-$(HE)_3$-DANS-ADAPT6-GSSC or MVDANS-ADAPT6-GSSC:	TTTTTTGGCGCGCCTTAACAGCTGCTACCGGGTAATGCATGTAAAATTTC	EILHALP**GSSC** Stop GAPK
MG-$(HE)_3$-DANS-ADAPT6-GGSC or MVDANS-ADAPT6-GGSC:	TTTTTTGGCGCGCCTTAACAGCTGCCACCGGGTAATGCATGTAAAATTTC	EILHALP**GGSC** Stop GAPK
MG-$(HE)_3$-DANS-ADAPT6-GGSSC or MVDANS-ADAPT6-GGSSC:	TTTTTTGGCGCGCCTTAACAGCTGCTGCCACCGGGTAATGCATGTAAAATTTC	EILHALP**GGSSC** Stop GAPK